

# Stability of beryllium coatings deposited on carbon under annealing up to 1073 K



R. Mateus<sup>a,\*</sup>, C. Porosnicu<sup>b</sup>, N. Franco<sup>a</sup>, P.A. Carvalho<sup>c,d</sup>, C.P. Lungu<sup>b</sup>, E. Alves<sup>a</sup>

<sup>a</sup> Instituto de Plasmas e Fusão Nuclear, Instituto Superior Técnico, Universidade de Lisboa, 1049-001 Lisboa, Portugal

<sup>b</sup> National Institute for Lasers, Plasma and Radiation Physics, Bucharest 077125, Romania

<sup>c</sup> SINTEF Materials Physics, Oslo, Norway

<sup>d</sup> CeFEMA, University of Lisbon, Instituto Superior Técnico, Lisbon, Portugal

## ARTICLE INFO

### Keywords:

Carbon  
Beryllium  
Reverse depositions  
Annealing  
Delamination

## ABSTRACT

Chemical reactions involving co-deposits in plasma facing components will occur under heat loads. Previous experiments in the Be-C-O system evidenced that compound formation may induce by itself the peel-off of deposits when C films are annealed in vacuum due to the simultaneous formation and mixing of Be<sub>2</sub>C and BeO. The present experiment investigates the reverse case, where Be films are deposited on graphite and annealed up to 1073 K. The delamination mechanism also exist and it is initialise at 973 K. However, it remains scarce since the carbide and oxide phases grow preferentially at different depths. The experiment points C as a source of dust in presence of Be in operative scenarios. Phase formation was followed by ion beam analysis, X-ray diffraction and electron microscopy.

## 1. Introduction

In the restricted group of elements with low neutron activation, beryllium (Be), carbon (C) and tungsten (W) were chosen as the main materials for plasma facing applications [1]. The erosion of the exposed plasma facing components (PFC), and the transport and co-deposition of impurities in other areas of the reactors imposes the formation of mixed materials and compounds under annealing in the surface of PFCs [1]. Power heat loads will promote the re-emission of the deposited material to the plasma as dust particles. Nevertheless, the same mechanism is enhanced when compound formation induces by itself the peel-off of the deposits, and therefore, it is important to study the chemical and thermal stability of the same materials at elevated temperatures. Compound formation was commonly studied with thin films in the absence of important amounts of oxygen (O). Nevertheless, the gathering of O may be significant as accidental impurity. Be and W tiles will be used in the first wall and divertor of ITER [2]. However, earlier designs included W coatings deposited on graphite based carbon fiber composites (CFC) for the target strike points of ITER divertor [1,2] and presently, CFC are still in use as support material for W coatings in the Joint European Torus (JET) tiles (W-CFC) [2]. The outcomes of the use of C in plasma reactors need to be fully reported and the research at IST involved the comparison of compound formation and stability of coatings within the Be-C-O and Be-W-O systems. The present document

is dedicated to the study of the first one, which was investigated in two reverse conditions: C deposited on Be plates and Be deposited on graphite.

Earlier studies evidenced that the diffusion of Be into C remains weak at 773 K with a diffusion rate of about 65 nm/h [3] (the corresponding diffusion coefficient is of  $2.9 \times 10^{-16}$  cm<sup>2</sup>/s). Nevertheless, the formation of beryllium carbide (Be<sub>2</sub>C) initializes at about 473 K in the Be-C interfaces [4] although it only becomes relevant within the 773 K–873 K temperature range [4]. Carbide formation may evolve at higher temperatures and depends of the morphology of the films [5]. The chemical stability of beryllium oxide (BeO) is deeply higher than that of Be<sub>2</sub>C, while the standard enthalpies of formation of BeO and of Be<sub>2</sub>C are -609 KJ/mol and -92.5 KJ/mol, respectively [6]. Therefore, and depending of the availability of O, the growth of the oxide tends to be favored over that of the carbide and is enhanced at higher temperatures. Typically, Be diffuses through the superficial layers, even through stoichiometric BeO, to oxidise at the surface [3–5]. At a base pressure of about  $5 \times 10^{-6}$  mbar, the formation of BeO is only enhanced at 873 K [5]. Once pure Be, graphite, BeO and Be<sub>2</sub>C have distinct stiffness, microstructures and thermal expansion coefficients, fracture and delamination in the Be-C co-deposits may occur under thermal stress [5,7,8]. Fractures are commonly enhanced in covalent bond and hard materials such as Be<sub>2</sub>C, or in ionic compounds like BeO which are stable and inert but also hard [7].

\* Corresponding author.

E-mail address: [rmateus@ipfn.ist.utl.pt](mailto:rmateus@ipfn.ist.utl.pt) (R. Mateus).

<https://doi.org/10.1016/j.fusengdes.2018.12.051>

Received 3 October 2018; Received in revised form 17 December 2018; Accepted 17 December 2018

Available online 04 January 2019

0920-3796/© 2019 The Authors. Published by Elsevier B.V. This is an open access article under the CC BY-NC-ND license (<http://creativecommons.org/licenses/by-nc-nd/4.0/>).

In a previous experiment, thin C coatings were evaporated on Be plates and annealed in vacuum in the temperature range 373 K–1073 K [5]. The only modification observed up to 773 K was the buckling of the C coatings occurred at low temperatures due to the low stiffness of the films. At the same time, the Be-C interdiffusion at the interface and the gathering of O at the surface remained very low. At 873 K a reaction front reached the edge of the buckling structures, where the addition of O is higher than that of the flat zones of the coatings. Possibly, BeO needs free space to growth due to the larger volume of the unit cell of BeO relatively to that of pure Be and it finds the additional space in the rough zones. At 973 K the reaction zone became spread out over the entire blisters surfaces, where the growth of the Be<sub>2</sub>C and BeO components is carried out along parallel lamellas via a discontinuous precipitation process. Be<sub>2</sub>C was found homogeneously distributed over the entire coating's surface, while most of BeO remains restricted to the buckles. Consequently, the hardness and distinct thermal expansion coefficients of Be<sub>2</sub>C and BeO led to the fracture and final peel-off of the buckles [5]. Evidences of the peel-off mechanism are shown at the end of Section 3 for a better discussion of the new data.

The fracture and the adhesion of Be-C coatings to the substrates depend of the depth profiles and mixing of the formed compounds. As a result, distinct delamination behaviour may occur in the reverse Be-C condition, i.e., when Be coatings are deposited on graphite plates, and this is the main study of the present experiment.

## 2. Experiment

Be coatings were deposited on polished graphite plates by thermionic vacuum arc (TVA) method [9]. The samples were annealed in vacuum with a base pressure close to  $5 \times 10^{-6}$  mbar in the temperature range 573 K to 1073 K using temperature steps of 100 K and time intervals of 90 min. Before and after the annealing procedure, X-ray diffraction (XRD) spectra were collected for phase identification making use of a Cu X-ray source and a grazing geometry. The X-ray diffraction patterns were identified from the ICDD database [10]. XRD patterns of light compounds as BeO or Be<sub>2</sub>C are difficult to achieve due to the predominant incoherent scattering of X-rays induced by light atoms [11] and minimum contents of BeO or Be<sub>2</sub>C are necessary for phase identification. The same feature makes impossible the identification of a Be pattern in the present thin films [11]. In opposition, ion beam analysis as Rutherford backscattering spectrometry (RBS) is particularly useful to detect Be in thin Be-C-O samples because all the individual elemental depth profiles are easily quantified by following the corresponding backscattering yields. In order to follow simultaneously the chemical reactivity of the layers by XRD and by RBS, the Be coatings were deposited on graphite with a nominal thickness of 150 nm. RBS spectra were collected using 2.0 MeV <sup>4</sup>He<sup>+</sup> incident ion beams and data analysis was performed with the NDF code [12].

Scanning electron microscopy (SEM) involving both secondary (SE) and backscattered electron (BSE) imaging as well as energy-dispersive X-ray spectroscopy (EDX) was carried out for topographic inspection and local chemical analysis. Typically, it is impossible to detect Be by EDX. However, O and C X-ray yields are easily identified, leading to the recognition of superficial BeO and of a C diffusivity (through the Be coatings) towards the surface at different temperatures. The INCA package software was used for the EDX elemental analysis [13]. The energy calibration of the EDX facility was carried out with the K $\alpha$  X-ray emissions of copper (8.05 keV) and of silicon (1.74 keV).

The thermal stability of the coatings may be discussed in face of physical and mechanical properties of the involved phases, as their thermal expansion and stiffness (expressed by the Young's modulus). Standard values for the linear thermal expansion coefficients  $\alpha$  and Young's modulus  $E$  of graphite ( $0.6\text{--}4.3 \times 10^{-6} \text{ K}^{-1}$  and 7 GPa), of Be<sub>2</sub>C ( $\sim 10.5 \times 10^{-6} \text{ K}^{-1}$  and 314 GPa) and of BeO ( $7.5\text{--}9.7 \times 10^{-6} \text{ K}^{-1}$  and 300 GPa) are presented in [14]. Corresponding values for Be are  $11.3 \times 10^{-6} \text{ K}^{-1}$  [14] and 303 GPa [15].

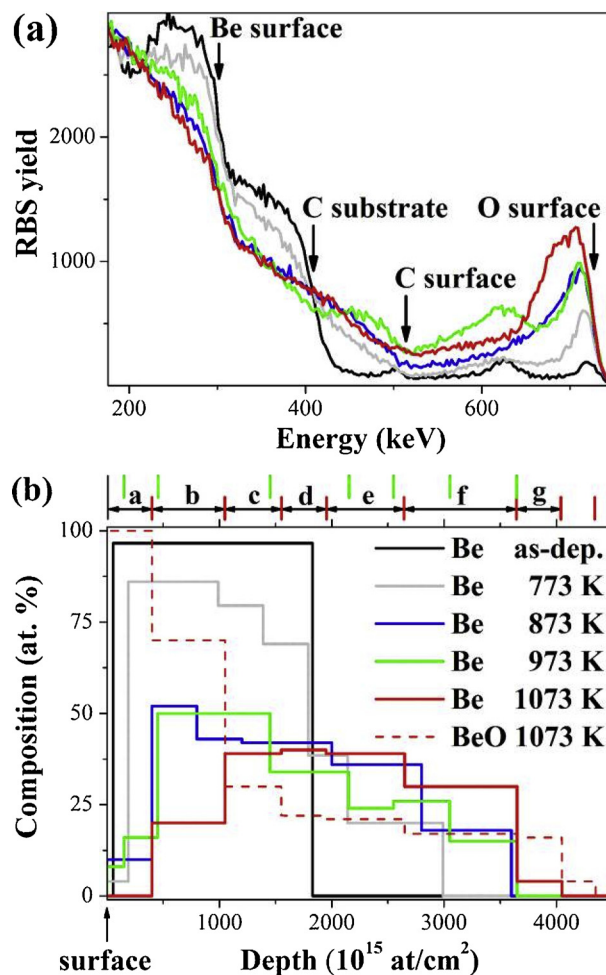


Fig. 1. RBS spectra (2.0 MeV <sup>4</sup>He<sup>+</sup> beams) collected from Be deposited on graphite before and after annealing (a) and related Be and BeO depth profiles (b). The depth range limits of the simulated layers (from a to g) are signalled on the top of figure (b) by the green (973 K) and red (1073 K) vertical lines (For interpretation of the references to colour in this figure legend, the reader is referred to the web version of this article).

## 3. Results and discussion

Fig. 1(a) presents RBS spectra collected from the Be coatings deposited on graphite. The energies signalling the presence of Be, C and O on the top of the superficial layers and of C on the C-Be interface are identified in the figure by vertical arrows. Due to the natural porosity of graphite plates, the Be films are not completely flat and a small amount of C is already visible on the top of the as-deposited sample. The presence of a superficial Be film leads to the recoil of the C backscattering yield. O is also present at the surface and at the C-Be interface in the same sample. The annealing route did not induce significant changes in the elemental depth profiles up to 673 K and at 773 K it is observed just a smooth decrease of the Be yield with a corresponding advance of the C yield towards the surface, revealing a weak intermixing between C and Be. The advance of the C yield, the C-Be mixing and the O content at the surface are extremely enhanced at higher temperatures. From 973 K to 1073 K it is also observed the recoil of the C yield, meaning that the presence of C on the surface is replaced at 1073 K by a new component. The simultaneous enhancement of the O yield suggests the growth of superficial BeO, as confirmed afterwards by XRD.

In face of the low enthalpy of formation of BeO relatively to that one of Be<sub>2</sub>C and assuming that all O reacts preferentially with Be, it is possible to evaluate a content for molecular BeO at the surface from the RBS data. As example, Fig. 1(b) presents the results for the depth profile

**Table 1**

Atomic depth profiles of BeO, Be<sub>2</sub>C and C after annealing at 973 K and 1073 K. The simulated layers (from a to g) agree with the depth range limits visualized on the top of Fig. 1(b).

Temp.	Phase	Composition of the simulated layers (at.%)						
		a	b	c	d	e	f	g
973 K	BeO	92	83	39	43	26	20	13
973 K	Be <sub>2</sub> C	8	17	61	37	19	40	10
973 K	C	0	0	0	20	55	40	77
1073 K	BeO	100	78	33	22	20	14	9
1073 K	Be <sub>2</sub> C	0	22	42	41	39	25	2
1073 K	C	0	0	25	37	41	61	89

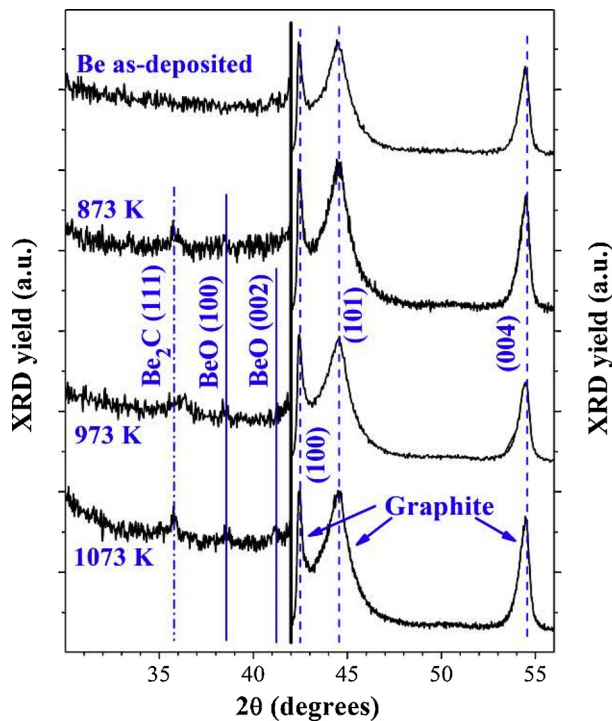


**Fig. 2.** XRD diffractograms of Be coatings deposited on graphite plates before and after annealing.

of BeO at 1073 K and for the remaining Be contents (apart BeO) during the annealing campaign. The depth composition of the films is completed by the C amounts (not presented). Assuming that non-oxidised Be reacts preferentially with C, final depth profiles for molecular BeO, Be<sub>2</sub>C and for C may be evaluated. Table 1 show the composition of the simulated layers after annealing at 973 K and 1073 K when the fracture events occur. Non-bounded Be revealed to be negligible. The results agree with a preferential growth of BeO at the surface and with the formation of Be<sub>2</sub>C at deeper depths.

From the XRD diffractograms of the as-deposited and annealed samples (Fig. 2) we observe the formation of Be<sub>2</sub>C from 873 to 1073 K, as identified by the characteristic diffraction line of plane (111) at 35.8°. The BeO pattern is also identified from 873 to 1073 K with the peak lines at 38.5 and 41.2° corresponding to planes (100) and (002). A pattern for the substrate material, graphite, is identified by the peak lines at 42.4°, 44.6° and 54.7° relative to planes (100), (101) and (004), respectively. All the RBS and XRD data are in agreement with the ones obtained from the reverse depositions, C deposited on Be plates [5], while the C-Be mixing and the growth of the carbide and oxide phases occur at similar temperatures [5]. In particular, the formation of Be<sub>2</sub>C is in agreement with the available data for the diffusivity of C on Be [3,4].

In opposition with the buckling mechanism observed in the reverse

depositions (C coatings deposited on Be plates) [5], the present annealing campaign did not promote the deformation of the Be coatings, which is explained by the high Young's modulus and stiffness of metallic Be, Be<sub>2</sub>C and BeO. Therefore, the addition of O arises homogeneously distributed in the surface at higher temperatures, while the same free volume necessary to the growth of BeO is disposed along the entire film. Be<sub>2</sub>C remains typically distributed at deeper depths along an extended C-Be interface (see Fig. 3 at 973 K). The segregation between the two phases mitigates the propagation of (cross-section) cracks under thermal stress within the coating's depth. Nevertheless, the C phase is fragile, and materials with high Young's modulus are hard and Be<sub>2</sub>C seems too brittle to prevent a very low but partial delamination of the coatings along the interface under thermal stress at 973 and 1073 K, due to the distinct thermal expansion coefficients of Be<sub>2</sub>C and graphite. Fig. 3(a) shows a SE tilted image of one of the few fracture events observed after annealing at 973 K. A top view of a delaminated area in the same coating and the corresponding EDS elemental maps for O and C are also presented in Fig. 3(b)–(d), respectively. The EDS results agree with the RBS data, while O is homogeneously distributed in the superficial layer and scarce at the substrate-coating interface as observed in the EDX mapping for O in Fig. 3(c), and C is quite restricted to the graphite substrate in the delaminated area as observed in the EDX mapping for C in Fig. 3(d). The EDX data reveal, once again, that the oxide and carbide phases grow preferentially at different depths. Typically, BeO is easily formed at the superficial layers and Be<sub>2</sub>C is mainly present along the interface.

The occurrence of delamination events in Be coatings deposited on graphite after annealing reveals to be scarce. The behaviour is completely distinct from that one observed in the reverse conditions, C films deposited on Be plates, where Be needs to diffuse through the C layer towards the surface to oxidise and a significant mixing between the BeO and Be<sub>2</sub>C phases occurs. In order to evidence the consequences arising by compound formation in this reverse case, additional SEM images and EDX elemental maps are presented in Fig. 4 for the same annealing temperature of 973 K. BeO grows preferentially in rough surfaces where the oxide (bright) and carbide (dark) phases segregate easily in a lamellar structure shown by the BSE image of Fig. 4(a), enhancing a severe peel-off mechanism due to different thermal and structural properties of BeO and Be<sub>2</sub>C. A peel-off event is presented in the SE image of Fig. 4(b). The corresponding EDX maps for O (d) and C (d) assures that BeO grows preferentially in rough topographies while Be<sub>2</sub>C is spread out along the entire surface [5].

The present work points compound formation as an important source for the delamination of thin coatings within the Be-C-O system due to thermal stress. This is evident in C films deposited on Be under annealing [5]. Nevertheless, the behaviour is highly mitigated when Be is deposited on CFCs. However, CFC surfaces easily present some porosity and C deposits in tokamaks also have irregular and porous morphologies [16] promoting the mixing of Be, C and O. Power heat loads in the reactor walls will result in further thermal stress and therefore, the emission of significant amounts of dust should be expected to occur in a Be-C environment.

The recent use of W coatings on CFC composites to achieve full metallic wall designs revealed to be a source for C contamination, and therefore the simultaneous formation of Be<sub>2</sub>C and BeO and related issues cannot be simply eliminated from modern tokamaks [17–19].

#### 4. Conclusions

CFCs are still in use in fusion devices and they may be a logic choice in some particular plasma applications. Earlier experiments with C coatings deposited on Be plates plus annealing evidenced a huge fracture and peel-off of the films after annealing at 973 K due to the simultaneous formation of hard BeO and Be<sub>2</sub>C disposed in lamellar structures along rough topographies. In the reverse case, Be coatings deposited on graphite, BeO forms in the surface of the flat films, and

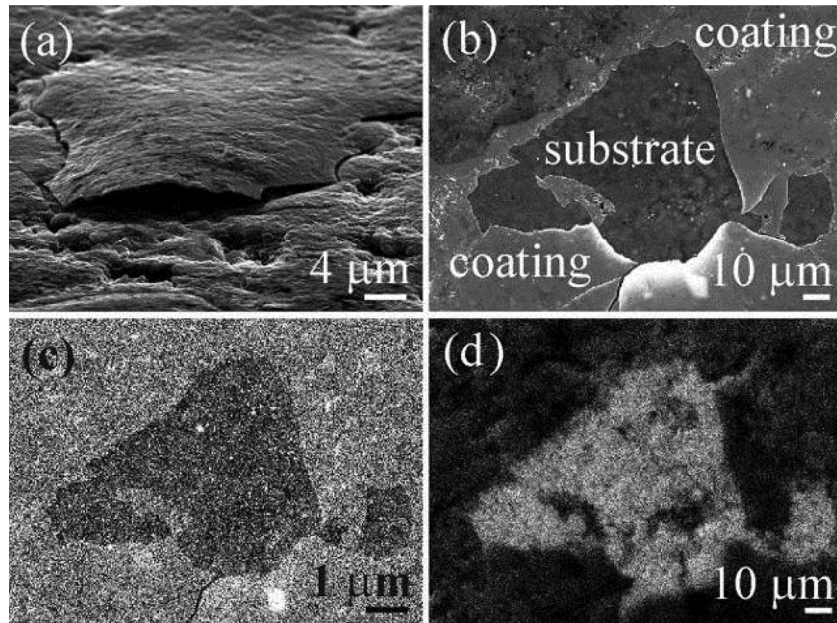


Fig. 3. SE tilted images of a fracture event (a) and top view of a delaminated area at 973 K (b); corresponding EDS maps for the K $\alpha$  emissions of O (c) and C (d).

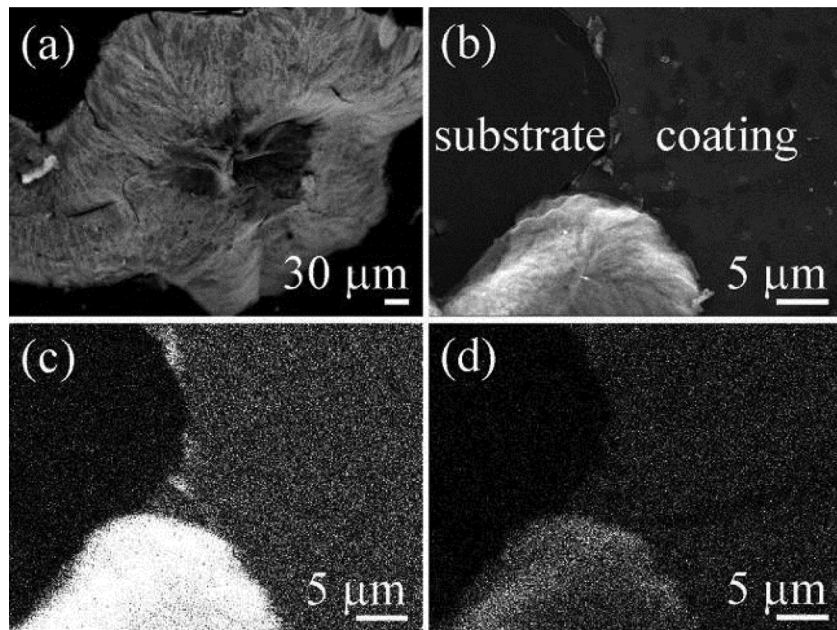


Fig. 4. C coating on Be after annealing at 973 K: BSE image of a blister/lamellar structure with Be<sub>2</sub>C and BeO (a), SE image of a peel-off event (b) and related EDS maps for O (c) and C (d).

Be<sub>2</sub>C grows mainly in an expanded C-Be interface. As a result, the oxide and carbide phases grow at distinct depth, mitigating issues caused by thermal stress as the peel-off events. However, C deposits in tokamaks present irregular morphologies, enhancing a Be<sub>2</sub>C and BeO mixing. Also the adhesion of hard Be-C coatings will decrease under power heat loads. The present investigation points the use of CFCs or of any accidental C impurity as an important source of dust emission to the main plasma in presence of a Be environment, while compound formation in the Be-C-O system induces by itself the fracture of co-deposits.

#### Acknowledgements

This work has been carried out within the framework of the EUROfusion Consortium and has received funding from the Euratom

research and training programme 2014-2018 under grant agreement No 633053. Work performed under EUROfusion WP PFC. The views and opinions expressed herein do not necessarily reflect those of the European Commission. IST also received financial support from FCT, Portugal, through project UID/FIS/50010/2013.

#### References

- [1] R.P. Doerner, *J. Nucl. Mater.* 363–365 (2007) 32.
- [2] C. Thomser, et al., *Fusion Sci. Technol.* 62 (2012) 1.
- [3] R.A. Anderl, et al., *J. Nucl. Mater.* 273 (1999) 1.
- [4] P. Goldstrass, et al., *J. Nucl. Mater.* 290–293 (2001) 76.
- [5] R. Mateus, et al., *J. Nucl. Mater.* 442 (2013) S320.
- [6] R.C. Ropp, *Encyclopedia of the Alkaline Earth Compounds*, Elsevier, Oxford, UK, 2013.
- [7] S. Zhang, et al., *Surf. Coat. Technol.* 198 (2005) 2.

- [8] S.A. Catledge, Y.K. Vohra, *Diamond Relat. Mater.* 9 (2000) 1327.
- [9] C.P. Lungu, et al., *Phys. Scr.* T128 (2007) 157.
- [10] JCPDS - International Centre for Diffraction Data, file numbers PDF #35-0818, PDF #33-0191.
- [11] B.D. Cullity, *Elements of X-ray diffraction*, second edition, Addison-Wesley, Reading, Massachusetts, USA, 1978.
- [12] N.P. Barradas, et al., *Appl. Phys. Lett.* 71 (1997) 291.
- [13] D. Li, et al., *J. Eur. Ceram. Soc.* 38 (2018) 1179.
- [14] W. Martienssen, H. Warlimont (Eds.), *Handbook of Condensed Matter and Materials Data*, Springer, Berlin, Heidelberg, New York, 2005.
- [15] A. Goldberg, *Atomic, Crystal, Elastic, Thermal, Nuclear, and Other Properties of Beryllium*, Technical Report LLNL UCRL-TR-224850, (2006).
- [16] M. Richou, et al., *Carbon* 45 (2007) 2723.
- [17] N. Catarino, et al., *Nucl. Mater. Energy* 12 (2017) 559.
- [18] M. Kumar, et al., *Nucl. Mater. Energy* 17 (2018) 295.
- [19] E. Fortuna-Zalesna, *Nucl. Mater. Energy* 12 (2017) 582.